

# Inhibition Effect of Pantoprazole Drug on Under-Deposit Corrosion of Carbon Steel

Roohangiz Morshedi, Mehdi Shahidi-Zandi\*, Maryam Kazemipour

Department of Chemistry, Kerman Branch, Islamic Azad University, Kerman, Iran.

\*E-mail: [meshahidizandi@gmail.com](mailto:meshahidizandi@gmail.com); [shahidi@iauk.ac.ir](mailto:shahidi@iauk.ac.ir)

Received: 28 April 2020 / Accepted: 26 August 2020 / Published: 31 October 2020

---

Inhibition effects of pantoprazole drug on the under-deposit corrosion of carbon steel in 3.5% NaCl solution saturated with CO<sub>2</sub> have been investigated by the techniques of potentiodynamic polarization and electrochemical impedance spectroscopy (EIS). The carbon steel electrode was covered with a layer of the silica sand to prepare the sand-covered electrode. The increase of the drug concentration led to an increase in the inhibition efficiency (IE) of carbon steel against under-deposit corrosion in the brine solution. The Langmuir isotherm can describe the adsorption behavior of pantoprazole on the surface of carbon steel. Measurements of potentiodynamic polarization indicated that pantoprazole is an anodic inhibitor. The effects of temperature on the under-deposit corrosion behavior of carbon steel were studied both in the absence and presence of pantoprazole drug. The enthalpy of the drug adsorption was obtained from the temperature dependence of the corrosion inhibition process. A reasonable agreement was observed between the IE values resulted from the potentiodynamic polarization and the EIS techniques.

---

**Keywords:** Pantoprazole; Under-deposit corrosion (UDC); CO<sub>2</sub> corrosion; Electrochemical impedance spectroscopy; Potentiodynamic polarization.

## 1. INTRODUCTION

The corrosion of steel pipelines of oil and gas increases by settling of deposits such as sand in them. It is very important to consider this type of corrosion, namely as the under-deposit corrosion (UDC), because of the pipeline leaking effect of it [1, 2].

Because of the presence of carbon dioxide gas in the oil wells, it is worth considering the CO<sub>2</sub> corrosion as a major challenge in the natural gas and oil industries [3-5]. The literature survey reveals a lot of papers on the CO<sub>2</sub> corrosion of steel alloys [3-14]. The CO<sub>2</sub> corrosion of the steel alloys has shown more severe corrosion in comparison with the same pH acidic solutions [14].

The main cathodic reactions in the CO<sub>2</sub> corrosion can be the reduction of H<sup>+</sup>, H<sub>2</sub>CO<sub>3</sub>, HCO<sub>3</sub><sup>-</sup> and H<sub>2</sub>O [15, 16]. Despite some debate in the literature, the hydrogen reduction reaction (HER) has been agreed as the predominant cathodic reaction at the pH range of 3 to 5.5 [17]. The Fe dissolution as the main anodic reaction involves an adsorbed intermediate as the rate-determining step [18].

The corrosion inhibitors, as the most common protecting materials for CO<sub>2</sub> corrosion of carbon steel [19], are substances whose small concentrations prevent the corrosion of the alloys by the corrosive media. The molecular structure of the most popular corrosion inhibitors contains S, N, O, P atoms and aromatic rings [20, 21]. The experiments of the sand adsorption have shown that the tendency of the corrosion inhibitors to adsorb on a sand substrate depends on their chemical nature [22, 23]. Sulfur-containing inhibitors indicate a lower tendency to adsorb on the sand substrate than to adsorb on the steel surface.

In this paper, pantoprazole drug was investigated as an inhibitor against the under-deposit corrosion of carbon steel in 3.5% sodium chloride solution saturated with CO<sub>2</sub> by the techniques of potentiodynamic polarization and impedance spectroscopy.

## 2. MATERIALS AND METHODS

### 2.1 Materials

Pantoprazole drug and silica sand (SiO<sub>2</sub>) were supplied from Sigma Aldrich. Sodium chloride was prepared from Merck. The molecular structure of the pantoprazole is shown in Figure 1. The working electrode used here is made of carbon steel with a surface area of 1.0 cm<sup>2</sup>.

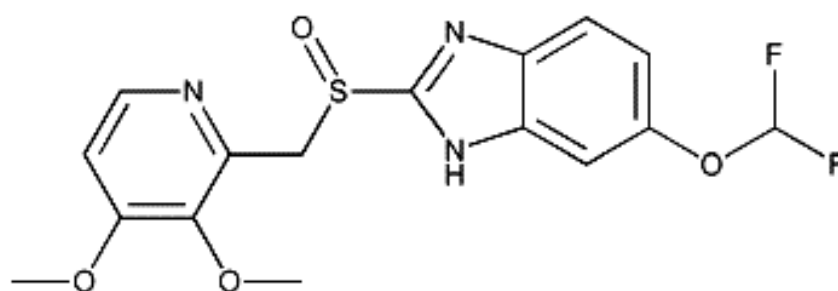


**Figure 1.** Structure of pantoprazole.

### 2.2 Methods

10 g of the acid-washed silica sand was used in all experiments. The working electrode (WE) was soaked in the CO<sub>2</sub> saturated brine solution. The WE was placed underneath a layer of silica sand to simulate the sand settling in the oil pipelines. The solutions under stagnant conditions were employed for the measurements.

The potentiodynamic polarization and impedance measurements were used to investigate the corrosion rate of carbon steel in the CO<sub>2</sub> saturated 3.5% sodium chloride solutions both in the absence

and presence of different amounts of pantoprazole drug. Before performing the tests, the surface of the sample was rubbed with wet sandpapers through different grades then washed with distilled water and at last dried in air. The sample, as the working electrode, was sealed by epoxy resin at one side after connecting a copper wire to it.

An Autolab 302N potentiostat equipped with Nova 1.9 software was used for potentiodynamic polarization and EIS tests. The counter electrode (CE) was prepared from a platinum rod and the reference electrode was a saturated (KCl) Ag/AgCl electrode. The electrochemical test order was EIS and afterward the polarization technique. Before performing the tests, the specimens were soaked in the solution for about 30 minutes to stabilize the open circuit potential (OCP).

For the EIS tests, a sinusoidal potential signal of 10 mV (vs OCP) was used in the frequency range of 100 kHz-10 mHz. Potentiodynamic polarization curves were obtained by changing the potential from -300 to + 300 mV vs. OCP with the scan rate of 1 mV/s. Nova 1.9 software was employed for both analyzing the Nyquist plots of EIS data and determining the polarization parameters arising from Tafel curves.

### 3. RESULTS AND DISCUSSION

#### 3.1 Polarization measurements

Figure 2 shows the potentiodynamic polarization plots of carbon steel exposed to CO<sub>2</sub> saturated NaCl solutions containing different amounts of pantoprazole. Since the cathodic branch displays a Tafel behavior it is possible to make an accurate evaluation of both the cathodic Tafel slope ( $\beta_c$ ) and the corrosion currents ( $j_{\text{corr}}$ ) by the Tafel extrapolation method [24]. On the other hand, the expected log/linear Tafel behavior is not displayed by the anodic polarization curve over the applied potential range. The deposition of the corrosion products or impurities in the carbon steel (e.g., Fe<sub>3</sub>C) and the formation of a non-passive film may be the reason for the curvature of the anodic branch [25]. Therefore, due to the curvature of the anodic branch, it is not suitable to evaluate the anodic Tafel slope by Tafel extrapolation of the anodic branch of the polarization plot.

In the Tafel extrapolation method, it preferred to use both the anodic and cathodic Tafel regions rather than only one Tafel region [26]. However, it is also possible to use the Tafel extrapolation of either the cathodic or anodic branch alone to determine the corrosion rate. In this condition, the cathodic branch is preferred due to the long defined Tafel region of it (as in our case here).

The anodic current density can be calculated from the experimental data. For this purpose, after extending the Tafel line of the cathodic branch to zero overvoltage, the following equation was employed to calculate the anodic current density [26]:

$$i_a(\text{net exp}) = i_a - |i_c| \quad (1)$$

where the subscripts a and c refer the anodic and cathodic terms, respectively. Thus, the anodic current density,  $i_a$ , is obtained from the sum of the net experimental anodic current density,  $i_a(\text{net exp})$ , and the extrapolated cathodic current density,  $|i_c|$ .

Table 1 lists the current density ( $i_{\text{corr}}$ ), the Tafel slopes ( $\beta_a$ ,  $\beta_c$ ) and corrosion potential ( $E_{\text{corr}}$ ).

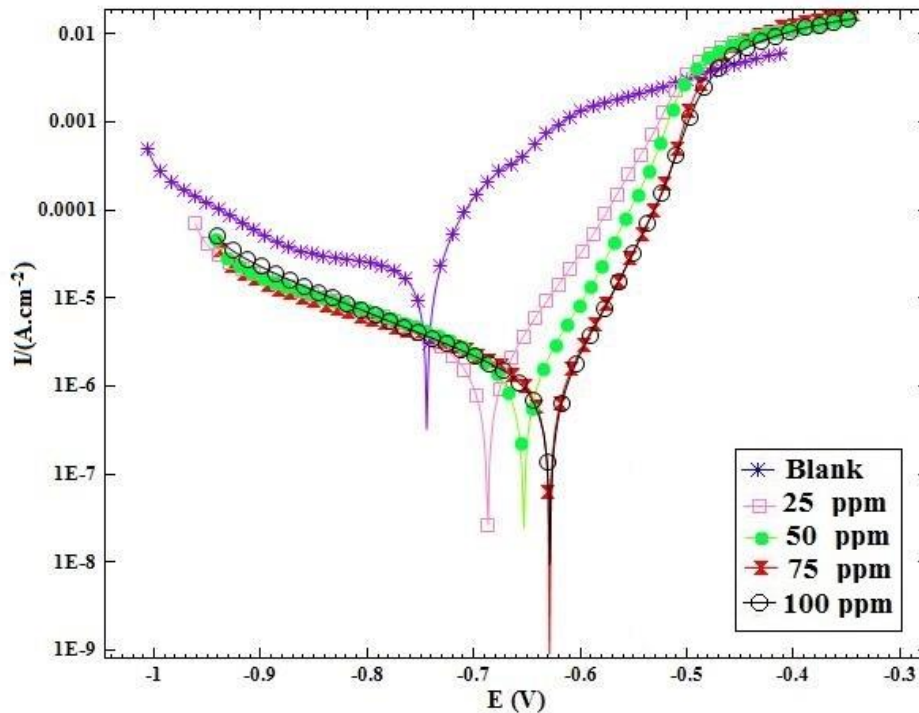


**Figure 2.** Polarization curves of carbon steel in CO<sub>2</sub> saturated brine solution containing different concentrations of pantoprazole at 25°C.

As it is clear from Figure 2, the anodic current density was found to decrease significantly after the addition of inhibitor, while the cathodic current density changed slightly after the inhibitor addition. Besides, it can be seen that the potential of corrosion changed to more positive values in the presence of inhibitor. Generally, the corrosion inhibitor will be considered as the cathodic or anodic type if the change in the absolute value of  $E_{corr}$  is more than 85 mV with respect to  $E_{corr}$  of the blank solution, and if the shift is less than 85 mV, the inhibitor can be classified as a mixed type [27-29]. In the present work, the maximum change in the equilibrium corrosion potential was +116 mV, suggesting that the pantoprazole can be known as an anodic inhibitor. This is in line with the above result stating that the anodic current density of the steel electrode in CO<sub>2</sub> saturated brine solution is significantly reduced by the addition of the inhibitor.

**Table 1.** Polarization parameters and the corresponding inhibition efficiencies for carbon steel in CO<sub>2</sub> saturated brine solution with different concentrations of pantoprazole at 25 °C.

C /ppm	$i_{corr}/\mu A.cm^{-2}$	$-E_{corr}/mV$	$\beta_a/mV.decade^{-1}$	$\beta_c/mV.decade^{-1}$	IE <sub>P</sub> (%)
0	22.4	745	95	464	-
25	3.5	687	61	264	84.4
50	2.5	653	49	259	88.8
75	1.9	630	43	250	91.5
100	1.6	629	44	193	92.9

Table 1 shows the inhibition efficiency (IE) values expressed by the following equation [30]:

$$IE_p(\%) = \frac{i_{corr} - i'_{corr}}{i_{corr}} \times 100 \quad (2)$$

where  $i_{corr}$  and  $i'_{corr}$  are current densities of corrosion in the blank and the inhibited solutions, respectively.  $IE_p$  values were enhanced by increasing the pantoprazole concentration and reached to 92.9% at 100 ppm of pantoprazole. These values indicate that the drug acts as an effective inhibitor for preventing the under-deposit corrosion of carbon steel at relatively low concentrations.

The surface coverage,  $\theta$ , can be calculated by  $\theta = IE(\%)/100$ . The isotherms of Langmuir, Frumkin, and Temkin were used for fitting data and the best results were found for Langmuir isotherm (Figure 3), which can be expressed in the following way [31]:

$$\frac{C}{\theta} = C + \frac{1}{K} \quad (3)$$

where  $C$  is the drug concentration,  $\theta$  is the surface coverage and  $K$  is the equilibrium constant of adsorption. As can be seen in Figure 3, the plot of  $C/\theta$  vs.  $C$  for the inhibitor is a linear plot with the correlation coefficient and slope close to 1, confirming the best fit of the polarization data to the Langmuir isotherm.

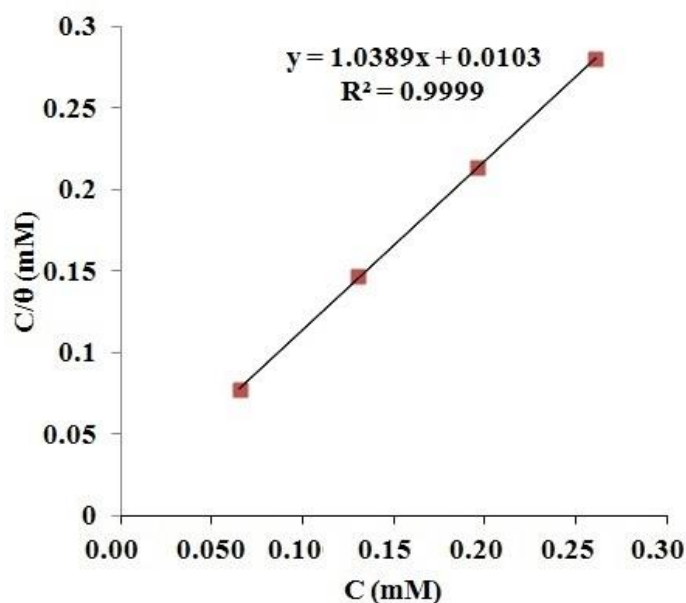


**Figure 3.** Langmuir adsorption isotherm of pantoprazole calculated by potentiodynamic polarization data for carbon steel in 3.5% NaCl solution saturated with  $CO_2$ .

### 3.2 Impedance measurements

The results of EIS measurements for carbon steel exposed to  $CO_2$  saturated brine solutions containing different amounts of pantoprazole are shown in Figure 4. The investigated electrochemical system has resistive and capacitive elements. This is due to the semi-circle form of the Nyquist diagrams. According to the Nyquist plots, the charge transfer resistance ( $R_{ct}$ ) increased with the

pantoprazole amount and reached its maximum value for 100 ppm of pantoprazole in the carbon dioxide saturated NaCl solution.

For investigating the details of electrochemical reactions occurring at the electrode/solution interface, an electrochemical equivalent circuit (Figure 5) was employed to fit the EIS results. Both a resistance of charge transfer ( $R_{ct}$ ) and a constant phase element ( $Q_{dl}$ ) were used in parallel to represent the corrosion process. The impedance value ( $Z_Q$ ) of  $Q_{dl}$  element can be determined by the following equation [32, 33]:

$$Z_Q = \frac{1}{Y_0(2\pi f j)^n} \quad (4)$$

where  $Y_0$  is the Q constant, n is the exponent of Q element and f is frequency. Table 2 lists the EIS parameters which are resulted from the fitting of Nyquist spectra to the proposed equivalent circuit.

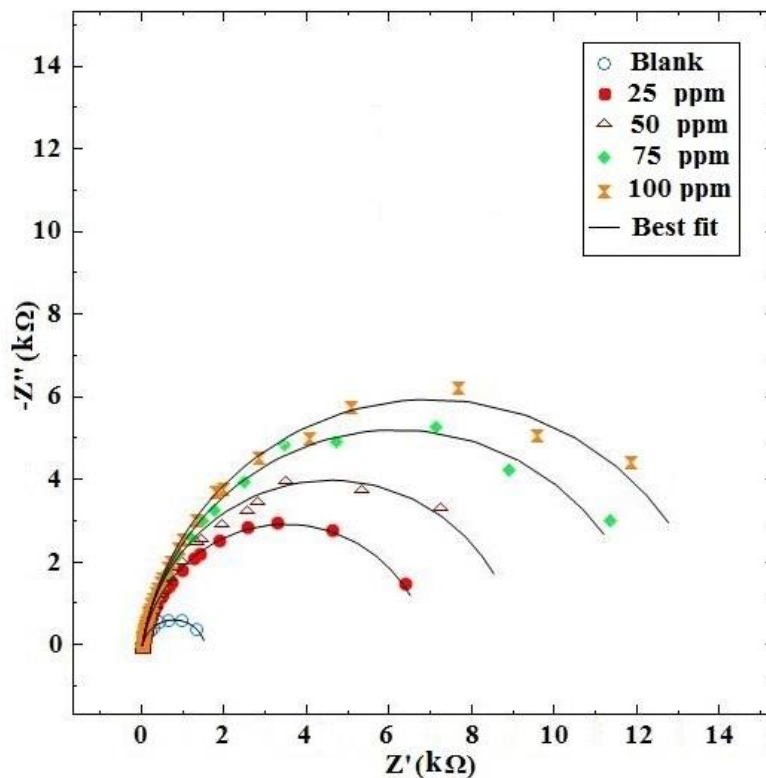


**Figure 4.** Nyquist plots for carbon steel in 3.5% NaCl solution saturated with  $CO_2$  containing different concentrations of pantoprazole at 25°C.

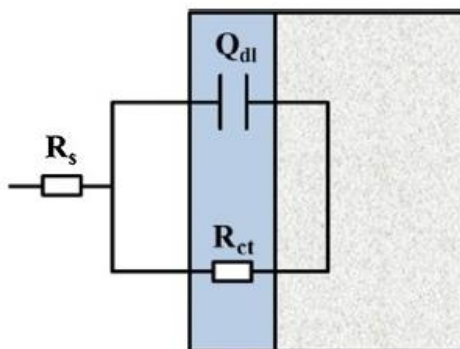


**Figure 5.** The equivalent circuit used to fit the experimental data.

**Table 2.** Impedance parameters arising from fitting the EIS data of Figure 4 and the corresponding inhibition efficiency values for carbon steel in CO<sub>2</sub> saturated brine solution at 25 °C.

C /ppm	R <sub>s</sub> /Ω.cm <sup>2</sup>	R <sub>ct</sub> /kΩ.cm <sup>2</sup>	n	10 <sup>6</sup> Y/Ω <sup>-1</sup> .cm <sup>-2</sup>	C <sub>dl</sub> /μF.cm <sup>-2</sup>	IE <sub>EIS</sub> (%)
0	9.4	1.5	0.872	83.5	60.8	-
25	9.5	7.1	0.896	42.7	37.9	78.9
50	8.7	9.2	0.918	35.6	32.4	83.7
75	6.8	12.5	0.896	31.3	29.3	88.0
100	10.1	15.3	0.900	26.7	25.1	90.2

The electrical double layer capacitance (C<sub>dl</sub>) was determined by the equation (5), providing the frequency of the maximum impedance imaginary component (f<sub>max</sub>) [34]:

$$C_{dl} = Y_0(2\pi f_{max})^{n-1} \tag{5}$$

It is evident from Table 2 that the increase of the drug concentration led to an increase in the R<sub>ct</sub> values and a decrease in the C<sub>dl</sub> values. This condition is due to the increased coverage of the steel surface by the drug, which can lead to decrease the aggressiveness of the CO<sub>2</sub> saturated brine solution. The IE% values in Table 2 were computed using the equation (6):

$$IE_{EIS}(\%) = \frac{R_{ct}' - R_{ct}}{R_{ct}'} \times 100 \tag{6}$$

where R<sub>ct</sub> and R<sub>ct</sub>' are the resistances of charge transfer for carbon steel in the CO<sub>2</sub> saturated brine solution before and after the addition of the drug, respectively. The increase of the drug concentration led to an increase in the IE values but there is a restriction in the sense that an additional increase in the drug amount did not make any considerable impact on the inhibition efficiency of the drug. This may be due to the saturation of the steel surface with the inhibitor molecules [35]. The impedance IE% values (Table 2) are completely consistent with the polarization IE% values (Table 1) and confirm each other.

The isotherms of Langmuir, Frumkin, and Temkin were employed for fitting the EIS data and the best results were found for Langmuir isotherm. As can be seen from Figure 6, the EIS results confirmed that the adsorption of pantoprazole molecules can be fitted well to the Langmuir isotherm because both the regression parameter and the slope values are notably close to 1.

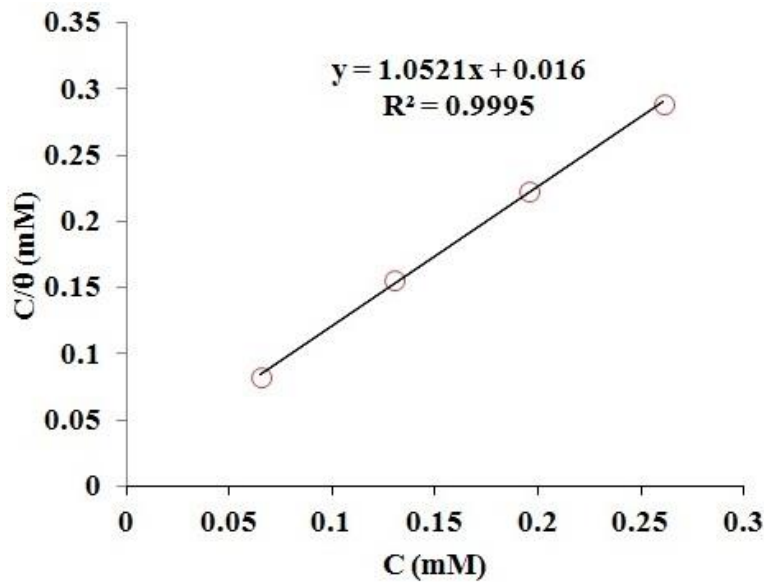


**Figure 6.** Langmuir adsorption isotherm of pantoprazole calculated on the basis of EIS data for carbon steel in 3.5% NaCl solution saturated with CO<sub>2</sub>.

### 3.3 The effect of temperature

Polarization measurements in the range of 25 to 55°C were used to determine the activation energy ( $E_a$ ) and some thermodynamic quantities for the carbon steel corrosion in the brine CO<sub>2</sub> saturated solution containing 100 ppm pantoprazole. The polarization curves for carbon steel exposed to the carbon dioxide saturated brine solutions in the blank solution and 100 ppm drug concentration are demonstrated in Figure 7.

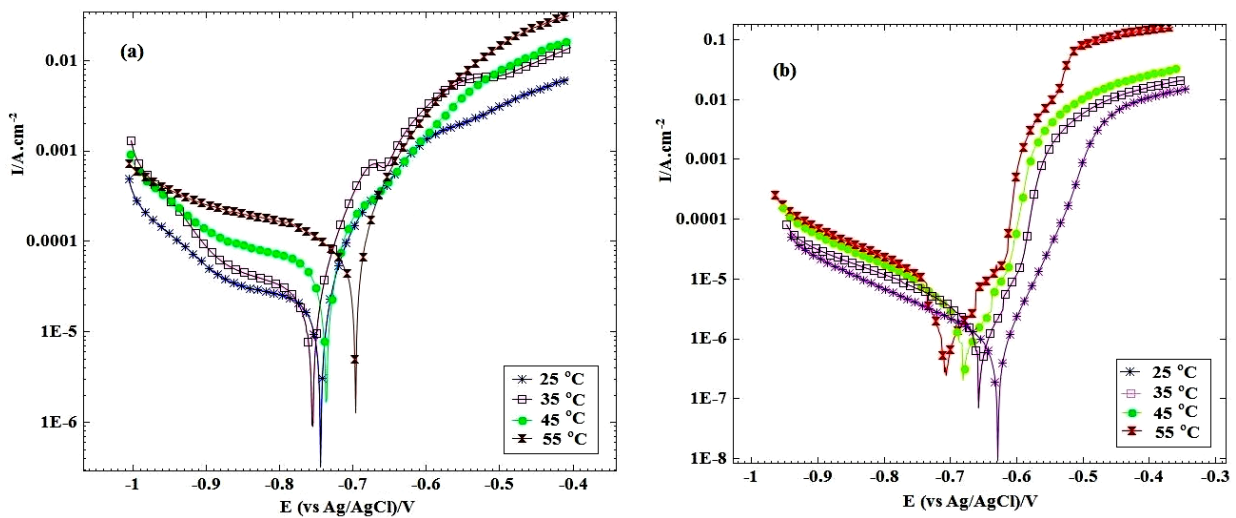


**Figure 7.** Effect of temperature on the polarization curves of carbon steel in CO<sub>2</sub> saturated brine solution (a) without pantoprazole drug and (b) in the presence of 100 ppm pantoprazole drug.

Table 3 lists the corrosion factors obtained at various temperatures. The results showed an increase in the current density with increasing temperature. Generally, the current density increases with increasing temperature due to the shortening of the time lag between the adsorption and desorption of inhibitor molecules on the steel surface with increasing temperature [36]. Therefore, the steel surface is exposed to the corrosive solution for a longer period, and thereby the corrosion rate of steel is increased with increasing temperature.

It is evident from the polarization results that with an increase in temperature, a decrease in IE% has happened. A slight change in the IE values with the rise of temperature from 25 to 55°C proves the strong adsorption bonding of pantoprazole on the steel surface. It means that besides physisorption, the chemisorption of pantoprazole should also be involved.

**Table 3.** Polarization parameters and the inhibition efficiencies, IE, obtained from polarization curves shown in Figure 7.

C/ppm	T/°C	$i_{corr}/\mu A.cm^{-2}$	IE%	$\theta$
<b>0</b>	25	22.4	-	-
	35	32.4	-	-
	45	45.3	-	-
	55	65.4	-	-
<b>100</b>	25	1.6	92.9	0.929
	35	2.7	91.7	0.917
	45	4.2	90.7	0.907
	55	7.1	89.1	0.891

Arrhenius equation can express the temperature influence on the corrosion rate according to equation (7):

$$i_{corr} = A \exp\left(\frac{-E_a}{RT}\right) \quad (7)$$

where  $i_{corr}$  is the corrosion current, A is the Arrhenius pre-exponential factor,  $E_a$  is the energy of activation, T is the temperature (K), and R is the molar gas constant ( $8.314 \text{ J K}^{-1}\text{mol}^{-1}$ ).  $E_a$  values can be obtained from the slope ( $-E_a/R$ ) of the Arrhenius plot [ $\ln i_{corr}$  vs  $1/T$ ]. Figure 8 shows the Arrhenius plots for carbon steel electrode in 3.5% NaCl solutions saturated with  $\text{CO}_2$  in the absence (blank) and the presence of pantoprazole. According to the slopes of the Arrhenius plots, it was revealed that the calculated  $E_a$  value in the presence of pantoprazole was larger than that in the absence of pantoprazole (40.1 kJ/mol vs 28.8 kJ/mol). The increase of  $E_a$  in the presence of pantoprazole indicates that the adsorption of pantoprazole on the steel surface leads to the formation of a physical barrier that reduces the steel reactivity in the electrochemical reactions of corrosion. Therefore, the rate of under deposit corrosion of carbon steel in the brine  $\text{CO}_2$  saturated solutions decreased by pantoprazole drug.

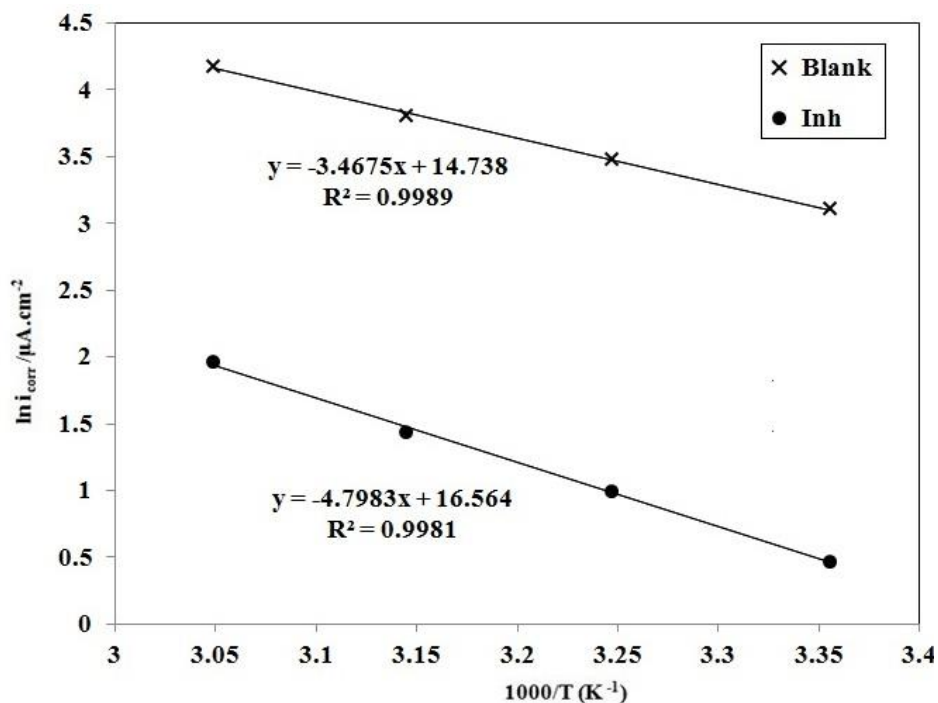


**Figure 8.** Arrhenius plots for carbon steel in CO<sub>2</sub> saturated brine solution in the absence (Blank) and presence of 100 ppm pantoprazole (Inh).

The following equation can be employed for calculation of the Gibbs energy of inhibitor adsorption ( $\Delta G_{ads}$ ) on the carbon steel:

$$\Delta G_{ads} = -RT \ln(55.5K_{ads}) \tag{8}$$

where T is the temperature (K), R is the gas constant and  $K_{ads}$  is the adsorption equilibrium constant. The reciprocal of the intercept of the Langmuir isotherm line is equal to the equilibrium constant of adsorption (Figure 3). The values of  $K_{ads}$  and  $\Delta G_{ads}$  are summarized in Table 4. Generally, if  $\Delta G_{ads}$  values are more positive than  $-20$  kJ/mol, it can be said that physical adsorption has occurred and if  $\Delta G_{ads}$  values are more negative than  $-40$  kJ mol<sup>-1</sup>, it can be said that chemical adsorption has occurred. Therefore, it can be concluded from the obtained value for  $\Delta G_{ads}$  (Table 4) that the adsorption of pantoprazole is not solely chemisorption or physisorption but involving comprehensive adsorption (both chemical and physical).

**Table 4.** The values of  $K_{ads}$  and  $\Delta G_{ads}$  obtained from the polarization and EIS data of carbon steel immersion in CO<sub>2</sub> saturated brine solution containing pantoprazole drug.

Drug	Polarizationl		EIS	
	$K_{ads}$ (M <sup>-1</sup> )	$\Delta G_{ads}$ (kJ.mol <sup>-1</sup> )	$K_{ads}$ (M <sup>-1</sup> )	$\Delta G_{ads}$ (kJ.mol <sup>-1</sup> )
Pan	97087	-38.4	62500	-37.3

The adsorption enthalpy,  $\Delta H_{ads}$ , can be computed by the equation (9) [31]:

$$\ln\left(\frac{\theta}{1-\theta}\right) = \ln A + \ln C - \frac{\Delta H_{ads}}{RT} \quad (9)$$

where  $\theta$  is the surface coverage calculated from  $\theta = IE(\%)/100$ ,  $A$  is a constant,  $C$  is the inhibitor concentration,  $R$  is the gas constant, and  $T$  is temperature. A straight line is obtained from the diagram of  $\ln(\theta/(1-\theta))$  vs  $1/T$  at the constant amount of the drug as shown in Figure 9. The line slope is equal to  $-\Delta H_{ads}/R$ . The calculated value of  $\Delta H_{ads}$  for the inhibitor adsorption is gathered in Table 5. The exothermic adsorption behavior of the drug on the steel surface can be understood from the negative value of  $\Delta H_{ads}$ .

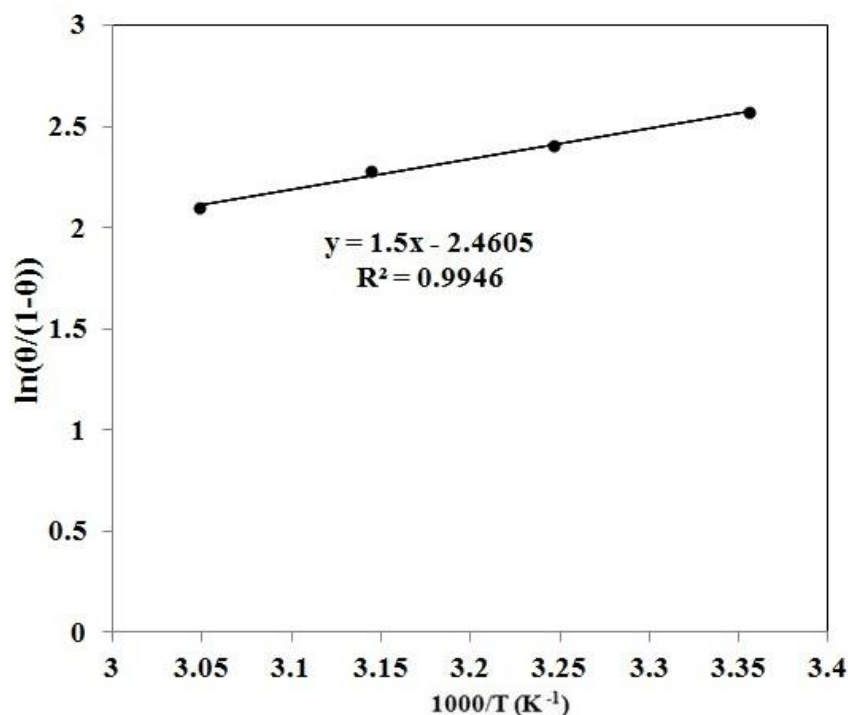


**Figure 9.** Plot of  $\ln(\theta/1-\theta)$  vs.  $1/T$  for carbon steel in  $\text{CO}_2$  saturated brine solution containing 100 ppm pantoprazole.

The following equation was employed to calculate the adsorption entropy ( $\Delta S_{ads}$ ):

$$\Delta G_{ads} = \Delta H_{ads} - T\Delta S_{ads} \quad (10)$$

The obtained value for  $\Delta S_{ads}$  is shown in Table 5. For accounting the negative value of  $\Delta S_{ads}$ , it should be noticed that the adsorption of drug molecules from the solution is a quasi-substitution process between the drug molecules in the solution and the adsorbed water molecules on the steel surface [37]. The adsorption of the drug on the carbon steel surface is accompanied by the desorption of water molecules from the steel surface [38]. Before the adsorption of the drug on the carbon steel surface, the drug molecules can move randomly in the bulk solution, while after adsorption, the drug molecules can adsorb orderly on the alloy surface, and then, a decrease in the adsorption entropy can occur.

**Table 5.** Activation and thermodynamic parameters of adsorption obtained by potentiodynamic polarization measurements for carbon steel in CO<sub>2</sub> saturated brine solution in the absence (Blank) and presence of 100 ppm of pantoprazole drug (Pan).

Drug	E <sub>a</sub> (kJ.mol <sup>-1</sup> )	K <sub>ads</sub> (M <sup>-1</sup> )	ΔG <sub>ads</sub> (kJ.mol <sup>-1</sup> )	ΔH <sub>ads</sub> (kJ.mol <sup>-1</sup> )	ΔS <sub>ads</sub> (J.K <sup>-1</sup> . mol <sup>-1</sup> )
Blank	28.8	-	-	-	-
Pan	39.9	97087	-38.4	-12.5	-87.0

### 3.4 Surface characterization

The optical microscope has been employed for evaluation of the effect of the drug on the surface morphology. The alloy specimens were immersed in the CO<sub>2</sub> saturated brine solutions both with and without 100 ppm drug concentration for 1 hour at room temperature. According to Figure 10, the steel specimen that was in contact with the drug showed a better condition in comparison to the one dipped in the blank solution. The specimen immersed in the drug solution showed less pitting corrosion in comparison with the blank sample. The steel surface was protected from corrosion due to the adsorption of the drug on the alloy surface.

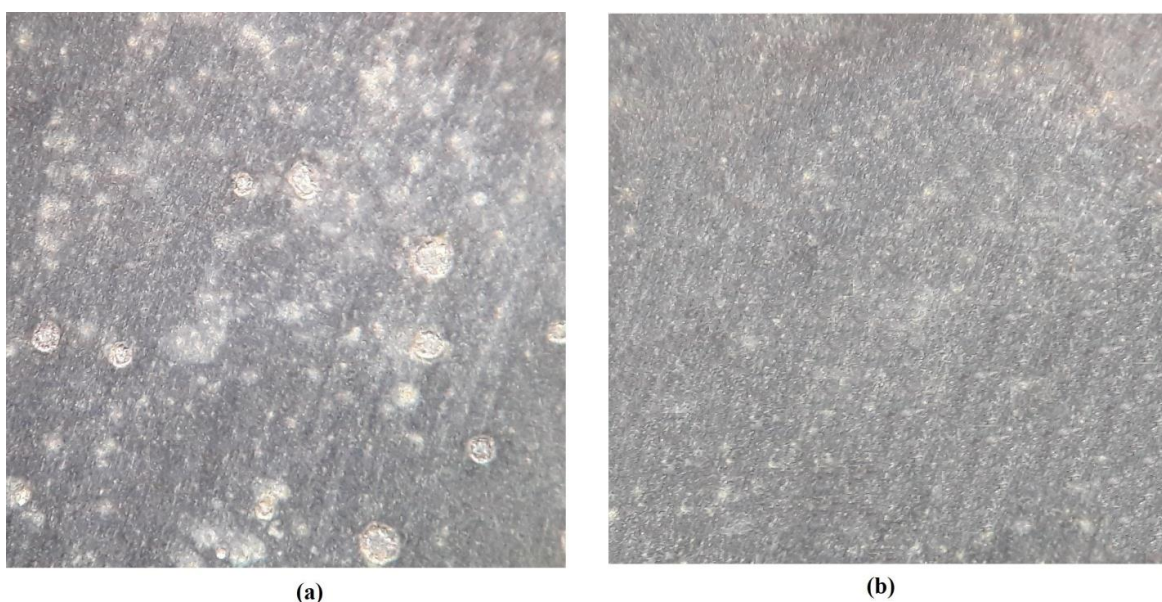


**Figure 10.** The optical microscopy images of sand-covered carbon steel electrode after 1 h from immersion in CO<sub>2</sub> saturated brine solution in (a) the absence and (b) presence of 100 ppm pantoprazole drug.

## 4. CONCLUSION

Pantoprazole drug was employed as an inhibitor for under-deposit corrosion protection of carbon steel in CO<sub>2</sub> saturated NaCl solution. potentiodynamic polarization curves showed that the drug reduced the corrosion of carbon steel. According to EIS measurements, the corrosion inhibition was

caused by an increase in the charge transfer resistance at the steel-solution interface. The data acquired from the potentiodynamic polarization and the impedance measurements indicated that the adsorption of pantoprazole on carbon steel in brine solution saturated with CO<sub>2</sub> follows the Langmuir isotherm. The potentiodynamic polarization experiments at different temperatures suggested that pantoprazole can effectively minimize the corrosion effects of solutions on the alloy surface. The reason for the inhibition of alloy by pantoprazole was due to the adsorption of pantoprazole molecules on the alloy surface which was also evidenced by Langmuir isotherm study. The IE and  $\Delta G_{\text{ads}}$  values obtained from the polarization method showed acceptable compatibility with the data acquired from the EIS technique.

## References

1. D. Han, R. J. Jiang, Y. F. Cheng. *Electrochim. Acta*, 114 (2013) 403.
2. Z. Mahidashti, M. Rezaei, M. P. Asfia. *Colloids and Surfaces A: Physicochemical and Engineering Aspects*, 602 (2020)
3. T. das Chagas Almeida, M. C. E. Bandeira, R. M. Moreira, O. R. Mattos. *Corros. Sci.*, 120 (2017) 239.
4. D. Dwivedi, K. Lepková, T. Becker. *RSC Advances*, 7 (2017) 4580.
5. R. F. Wright, E. R. Brand, M. Ziomek-Moroz, J. H. Tylczak, P. R. Ohodnicki. *Electrochim. Acta*, 290 (2018) 626.
6. D. A. Lopez, S. N. Simison, S. R. d. Sanchez. *Electrochim. Acta*, 48 (2003) 845.
7. X. Jiang, S. Nešić. *Corrosion/2009*, Paper No. 2414, NACE, Houston, TX (2009)
8. X. Jiang, S. Nestic, F. Huet, B. Kinsella, B. Brown, D. Young. *J. Electrochem. Soc.*, 159 (2012) C283.
9. S. N. Esmaeely, Y.-S. Choi, D. Young, S. Nešić. *CORROSION*, 69 (2013) 912.
10. W. Li, B. Brown, D. Young, S. Nešić. *CORROSION*, 70 (2014) 294.
11. R. D. Motte, R. e. Mingant, J. Kittel, F. Ropital, P. Combrade, S. Necib, V. Deydier, D. Crusset. *Electrochim. Acta*, 290 (2018) 605.
12. A. Kahyarian, B. Brown, S. Nestic. *Corros. Sci.*, 129 (2017) 146.
13. S. Hatami, A. Ghaderi-Ardakani, M. Niknejad-Khomami, F. Karimi-Malekabadi, M. R. Rasaei, A. H. Mohammadi. *The Journal of Supercritical Fluids*, 117 (2016) 108.
14. B. R. Linter, G. T. Burstein. *Corros. Sci.*, 41 (1999) 117.
15. J. Han, J. Zhang, J. W. Carey. *Int. J. Greenh. Gas Con.*, 5 (2011) 1680.
16. U. Bharatiya, P. Gal, A. Agrawal, M. Shah, A. Sircar. *Journal of Bio- and Tribo-Corrosion*, 5 (2019) 35.
17. R. A. D. Motte, R. Barker, D. Burkle, S. M. Vargas, A. Neville. *Mater. Chem. Phys.*, 216 (2018) 102.
18. R. Feng, J. Beck, M. Ziomek-Moroz, S. N. Lvov. *Electrochim. Acta*, 212 (2016) 998.
19. M. Javidi, R. Chamanfar, S. Bekhrad. *Journal of Natural Gas Science and Engineering*, 61 (2019) 197.
20. H. H. Zhang, Y. Chen. *J. Mol. Struct.*, 1177 (2019) 90.
21. M. R. Gholamhosseinzadeh, H. Aghaie, M. Shahidi Zandi, M. Giahi. *J. Mater. Res. Technol.*, 8 (2019) 5314.
22. V. Pandarinathan, K. Lepková, S. I. Bailey, R. Gubner. *Corros. Sci.*, 72 (2013) 108.
23. V. Pandarinathan, K. r. Lepková, S. I. Bailey, R. Gubner. *J. Electrochem. Soc.*, 160 (2013) C432.

24. R. Samiee, B. Ramezanzadeh, M. Mahdavian, E. Alibakhshi. *Journal of Cleaner Production*, 220 (2019) 340.
25. M. A. Amin, M. M. Ibrahim. *Corros. Sci.*, 53 (2011) 873.
26. E. McCafferty. *Corros. Sci.*, 47 (2005) 3202.
27. Y. Liang, C. Wang, J. Li, L. Wang, J. Fu. *Int. J. Electrochem. Sci.*, 10 (2015) 8072.
28. S. Hari Kumar, S. Karthikeyan. *Ind. Eng. Chem. Res.*, 52 (2013) 7457.
29. M. Lebrini, F. Robert, H. Vezin, C. Roos. *Corros. Sci.*, 52 (2010) 3367.
30. V. S. Sastri, *Green Corrosion Inhibitors; Theory and Practice*, John Wiley & Sons, (2011) New Jersey.
31. G. Golestani, M. Shahidi, D. Ghazanfari. *Appl. Surf. Sci.*, 308 (2014) 347.
32. M. G. Hosseini, M. Ehteshamzadeh, T. Shahrabi. *Electrochim. Acta*, 52 (2007) 3680.
33. M. Mobin, M. Basik, J. Aslam. *Measurement*, 134 (2019)
34. Z. Golshani, S. M. A. Hosseini, M. S. Zandi, M. J. Bahrami. *Mater. Corros.*, 70 (2019) 1862.
35. I. Rotaru, S. Varvara, L. Gaina, L. M. Muresan. *Appl. Surf. Sci.*, 321 (2014) 188.
36. E. A. Noor. *Corros. Sci.*, 47 (2005) 33.
37. I. Ahamad, R. Prasad, M. A. Quraishi. *Corros. Sci.*, 52 (2010) 933.
38. M. Şahin, S. Bilgiç, H. Yılmaz. *Appl. Surf. Sci.*, 195 (2002) 1

© 2020 The Authors. Published by ESG ([www.electrochemsci.org](http://www.electrochemsci.org)). This article is an open access article distributed under the terms and conditions of the Creative Commons Attribution license (<http://creativecommons.org/licenses/by/4.0/>).